Singularities in five-axis machining: cause, effect and avoidance.

R. J. Cripps, B. Cross, M. Hunt and G. Mullineux

Abstract

Singular configurations of five-axis machines have long been observed. Machining near to such singularities drastically affects the behaviour of machine axes movements. Singularities have been linked to the kinematic chain of the machine configuration but not necessarily machine axes movement. The first contribution of this paper is a link between cutter motion in workpiece and machine coordinate systems. This leads to a description for the machine axes movements for a given tool path. Unstable machine axes movements are discovered near singular configurations of the rotary axes. By relating these configurations to orientations in the workpiece coordinate system, a simple approach that avoids singularities by reorienting the workpiece is proposed. Machining tests verify the effectiveness of this approach.

Keywords: five-axis machine tool, singularity

1. Introduction

Many modern products are now designed and manufactured entirely within the computer aided design and manufacture (CADCAM) environment. The process begins with the design of a product within some CAD software. This computerised model is then transferred to the CAM software wherein the

machining strategy is determined. The CAM software is used to generate a sequence of tool paths which when implemented on a CNC machine tool result in the final component.

Depending upon what type of CNC machine tool is to be used, different types of tool paths can be generated. Conventional three-axis machining, with three linear axes, accommodates numerical control of the cutter position. The addition of two rotary axes in five-axis machining offers the extra capability to control orientation of the cutter. This added flexibility can be utilised to machine more complex geometries, reduce the number of set-ups, achieve higher material-removal rates, improve surface finish and thus increase productivity [1].

A drawback to using rotary axes is that problems can arise in accurately controlling the cutter position on the workpiece (material block). Physical motions of the actual cutter can significantly differ from that of the CAM tool path simulation. This is due partly to the non-linearity of cutter movement between the points specified by the NC code [2] and partly to dynamical effects such as high jerk [3]. Dynamical abnormalities affect the surface finish of the final component and can lead to undesired gouges. Consequences of this disconnection, between the desired motion from the CAM model and the actual motion of the cutter, are more noticeable near singular configurations of the machine tool.

Mechanical singularities occur in configurations where subsequent behaviour becomes less predictable. Zlatanov et al. [4] define the occurrence of a *redundant input* singularity when there exists a non-zero input for a machine that yields a zero output. Singular configurations of five-axis machine

tools are redundant in this sense in that the output, i.e. the cutter position and orientation, is unaffected by certain inputs, i.e. axes movements. Singularities of five-axis machines are linked to the inverse kinematics of the machine configuration. Every five-axis machine (with three linear and two rotary axes) possesses a redundant input singularity (section 2.4).

All of the configurations that are within some tolerance of a singularity form a singular region. When machining with configurations inside a singular region, undesired machine behaviour is observed [6]. This manifests itself as a sharp variation in machine axes movements in an attempt to attain constant cutting feed rate. The majority of research explains the effect of such undesired behaviour based upon observational results. The reasons why singular configurations of five-axis machine tools cause this behaviour however have not been investigated until recently.

One such investigation considered the orientation changes within a CAM tool path [5]. Orientations of the cutter are represented as vectors from the center to the surface of the unit sphere. Differences between them are measured with respect to the angle between the vectors. Using the kinematic chain, corresponding rotary axes movements are derived for different orientation changes. An asymptotic behaviour is inferred and shown to correlate with the singularity.

The first contribution of this paper extends the analytical ideas of [5] from a finite difference model into an infinitesimal difference model i.e. using derivatives. Further to this, by relating the coordinate systems for the CAM model and machine tool, it is possible to model the machine axes movements for a given CAM tool path. Calculus between these coordinate systems is

derived to predict machine axes movement. The second contribution uses insight from the derived equations to create a novel singularity avoidance strategy.

Existing research into singularities of five axes machine tools generally falls into two distinct categories: management and avoidance. In [2] the onus of safely traversing the singularity is managed in the post-processing stage. To ensure that the traversal of the cutter is within a suitable tolerance of the desired tool path, the sampling rate is increased in the local neighbourhood of the singularity. Although a greater accuracy of control is achieved, slowing of the cutting feed rate is observed. Consequences of this behaviour can be an increase in machining time and undesirable cutter dwell marks.

Lin et. al. [5] argue that in theory it is possible to pass through the singularity and not induce any undesirable machine behaviour. This is achieved by manipulating the tool path local to the singularity so that only the primary rotary axis is moving. This results in a tool path in which the orientations on the boundary of a singular region must satisfy geometrical constraints. As explained in [5], this restriction is not practical.

In terms of singularity avoidance strategies, a manipulation of the tool path at the CAM stage is the most common approach. By describing the tool positions and orientations in terms of B-spline curves, local manipulations to avoid a singular region are achieved by moving appropriate control points [6]. A similar technique that uses geometric algebra to describe orientations is presented in [7]. Traditional B-splines are used to describe the position of the tool tip as well as B-splines in quaternions for orientations. The quaternion B-splines are manipulated to avoid entering a singular region.

Another singularity avoidance strategy transforms the cutter orientations onto the unit sphere and offsets them in this space to again avoid a singular region [5].

The approach in [8] is different in that each tool position is associated with a range of orientations (domain of admissible orientations). A tool path is found by selecting orientations from these domains through optimisation of cost functions taking into account singularity avoidance. The drawbacks of all these singularity avoidance strategies are discussed in detail in Section 3.1.

In outline this paper is organised as follows. Section 2 explains the cause of undesired machine axes behaviour due to traversing near to a singularity. This is achieved by examining machine axes movements for a given tool path motion. Two coordinate systems are introduced to distinguish between the CAM tool path and machine motion. Changes in orientation of the cutter are examined in the different coordinate systems. Relating these changes to movements of the machine axes explains the behaviour observed near to the singularity.

Section 3 uses insight from the cause of singular behaviour to create a novel singularity avoidance strategy. The drawbacks of existing approaches are discussed first and linked to the common theme of trying to manipulate the tool path in the CAM stage. It is shown that reorientating the workpiece on the table affects the machine configuration in an easily comprehensible manner. Reorientation is then used as a strategy which can transform machine configurations away from the singularity. In Section 4 the effectiveness of the reorientation procedure is investigated with machining experiments.

The paper finishes with some conclusions into what new insight has been gained into singularities and avoidance strategies.

2. Cause of undesired machine axes behaviour

This section examines what causes the singular behaviour observed local to the singularity. The observation is a sharp variation in machine axes movements at constant cutting feed rate. Separate coordinate systems, associated with the CAM simulation and the machining stage, are presented for subsequent analysis. Since the interest lies in the rate of movement, calculus on the two coordinate systems is used. Interpretation of the calculus leads to an improved understanding of singular behaviour.

2.1. Workpiece and machine coordinate systems

The tool paths generated in CAM software are designed to be independent of the machine tool and are defined in a coordinate system relative to the workpiece. However the machine tool is controlled using a machine coordinate system, where axis values are defined relative to fixed parts of the machine. The two coordinate systems are connected via a kinematic chain of transformations. The analysis presented here takes on a specific kinematic chain for illustration. Other machine configurations follow similar analysis as outlined in section 2.4.

The kinematic chain introduced here is based on the Hermle C600U machine tool [9]. The five axes consist of three translational axes (X, Y, Z) controlling spindle position and two rotary axes (A, C) controlling the orientation of the workpiece. The workpiece is fixed onto a rotary table (C-axis)

that is attached to a tilting table (A-axis) at the lower part of the machine (Figure 1).

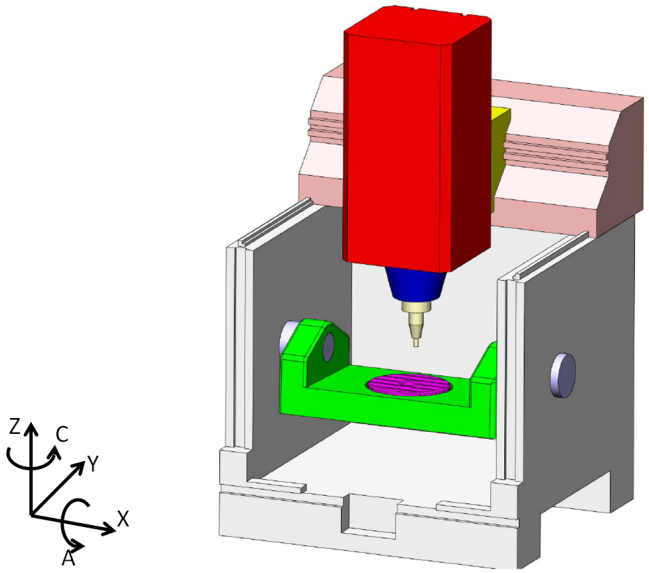

Figure 1: Schematic of the Hermle C600U machine tool.

The *workpiece coordinate system*, $\mathbf{P}_W = (x, y, z)$, and *machine coordinate system*, $\mathbf{P}_M = (X, Y, Z)$, have their origins defined as the intersection of the axes of rotations for the A and C rotary axes. The (X, Y, Z) directions of the machine coordinates align with the (X, Y, Z) translational movements along their corresponding guide-ways. When the A and C rotary axes are set to zero the (x, y, z) directions in the workpiece coordinate system agree with the machine coordinate system.

The relationship between the position in the workpiece space and machine space can be derived from the kinematic chain connecting the two coordinate

systems:

$$\mathbf{P}_W = \begin{pmatrix} x \\ y \\ z \end{pmatrix} = \begin{pmatrix} \cos(C) & \sin(C) & 0 \\ -\sin(C) & \cos(C) & 0 \\ 0 & 0 & 1 \end{pmatrix} \begin{pmatrix} 1 & 0 & 0 \\ 0 & \cos(A) & \sin(A) \\ 0 & -\sin(A) & \cos(A) \end{pmatrix} \begin{pmatrix} X \\ Y \\ Z \end{pmatrix}$$

$$= \mathbf{R}_z(C)\mathbf{R}_x(A)\mathbf{P}_M$$

$$\Rightarrow \mathbf{P}_M = \mathbf{R}_x(-A)\mathbf{R}_z(-C)\mathbf{P}_W \tag{1}$$

Here A and C are the angles of the rotary axes and $\mathbf{R}_i(j)$ is the rotation matrix along the i axis of angle j.

In machine space the cutter is always aligned in the Z-direction. However in workpiece space the cutter orientation depends upon the angles of the rotary axes. A unit vector, $\mathbf{O}_W$, is used to describe this orientation. This relationship is given by:

$$\mathbf{O}_W = \mathbf{R}_z(C)\mathbf{R}_x(A)\mathbf{O}_M = \begin{pmatrix} \sin(C)\sin(A) \\ \cos(C)\sin(A) \\ \cos(A) \end{pmatrix} \tag{2}$$

where $\mathbf{O}_M = (0, 0, 1)^T$. Given a desired orientation of the cutter relative to the workpiece, $\mathbf{O}_W$, the corresponding angles of the rotary axes can be found by solving equation (2).

Use $\tan^{-1}(y, x)$ to denote the arctangent function (as in programming languages) which yields $\tan^{-1}(y/x)$ with due allowance for the appropriate quadrant and for the case when x is zero. Then $\sin(A) = \pm\sqrt{i^2 + j^2}$ and

$$A = \tan^{-1}(\pm\sqrt{i^2 + j^2}, k)$$

$$C = \tan^{-1}(\pm i, \pm j) \qquad \text{if } i \text{ and } j \text{ are both non-zero}$$

$k = +1$	$A = 0$	C - undefined
$k = -1$	$A = \pi$	C - undefined
$-1 < k < 1$	$A = \tan^{-1}(\pm\sqrt{i^2 + j^2}, k)$	$C = \tan^{-1}(\pm i, \pm j)$

Table 1: A and C angles for a given orientation $\mathbf{O}_W = (i, j, k)$.

The sign choice reflects the two possible solutions (when $\sin(A) \neq 0$). If one of the solutions is A and C, then another solution consists of $-A$ and $C + \pi$. If $\sin(A)$ is zero, then so are i and j, and hence C is undefined and can take any value. In this case $k = \pm 1$. It is seen that, if $k = +1$, then $A = 0$, and if $k = -1$, then $A = \pi$.

Table 1 summarizes the possible pairs of solutions. This is the equivalent of Table 1 in [6] except that in the paper the choice of signs for the square roots is not explicitly presented.

In practice, it seems unlikely that the range of values of angle A can be large. It seems reasonable to assume that $-\frac{\pi}{2} \leq A \leq \frac{\pi}{2}$, or else the bed of the machine is starting to turn completely over. This means that $0 \leq k \leq 1$.

Certain orientations correspond to a singularity. These are identified when orientations are ill-defined, as is the case when $\mathbf{O}_W = (0, 0, 1)^T$. This is due to the fact that when the cutter is oriented at $(0, 0, 1)^T$ it is possible to spin the C-axis and follow the circle in the XY plane centered on the C-axis of rotation without affecting the output, i.e. position and orientation of the cutter with respect to the workpiece.

The effect of traversing near to singular configurations is a rapid change in machine axes movements [6]. To identify what causes this, the speed of machine axes movements is modelled. In order to do this the position and

orientation of the cutter are differentiated with respect to time.

2.2. Calculus of tool path motions

Differences between orientations must be quantified in order to measure speed of orientation change. In the workpiece coordinate environment this measurement, Θ, corresponds to the difference in angle between two orientations, $\mathbf{O}_1$ and $\mathbf{O}_2$, and can be written as

$$\Theta(\mathbf{O}_1, \mathbf{O}_2) = \angle(\mathbf{O}_1, \mathbf{O}_2) = \arccos(\mathbf{O}_1 \cdot \mathbf{O}_2).$$

Visualising $\mathbf{O}_1$ and $\mathbf{O}_2$ as points on the sphere, $\Theta(\mathbf{O}_1, \mathbf{O}_2)$ corresponds to the length of the great arc segment connecting the two points on the sphere.

This description of change in orientation is not necessarily consistent with how a machine tool interprets orientations. To see this, a relationship between Θ and the rotary axes is derived. To visualise this connection between $\mathbf{O}_W$ and the A and C values consider associating the vector $\mathbf{O}_W$ with a point on the unit sphere. It is now shown that the A and C values correspond to the longitudinal and latitudinal components of $\mathbf{O}_W$ respectively.

To show this consider moving a reference point from the north pole along the unit circle in the yz plane through an angle A to a new point on the sphere ($\mathbf{O}_V$). This forms its vertical or *longitudinal* component (Figure 2). Now move this point along the horizontal circle through an angle C. This movement defines the horizontal or *latitudinal* position (Figure 2). This process is equivalent to starting with $\mathbf{O}_M = (0, 0, 1)^T$ applying the rotation matrix $\mathbf{R}_x(A)$ to get $\mathbf{O}_V$ and then applying $\mathbf{R}_z(C)$. From (2) it is apparent that the new vector corresponds to $\mathbf{O}_W$.

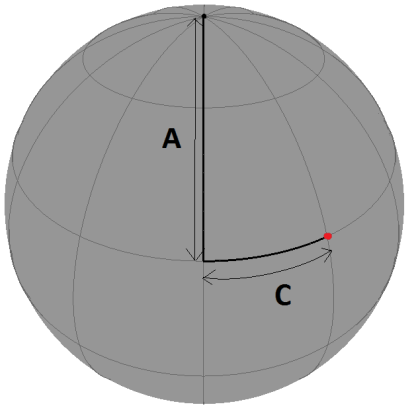

Figure 2: The cutter orientation with respect to machine parameters A and C visualised on the unit sphere.

To see how a change in Θ affects the A and C rotary axes the derivative terms representing this change, $\dfrac{\partial\Theta}{\partial A}$ and $\dfrac{\partial\Theta}{\partial C}$ respectively, need to be determined. This is done using geometric arguments.

Consider the orientation vector changing as a function of time, i.e. $\mathbf{O}_W(t)$ for $t \in [t_0, t_1]$. The total orientation change can be found by summing the speed of orientation change over time. This can be written as

$$\Theta(t_0, t_1) = \int_{t_0}^{t_1} ||\dot{\mathbf{O}}_W||\, dt$$

which corresponds to the length of the path traced out by $\mathbf{O}_W(t)$ on the sphere.

The derivative vector describing orientation change, $\dot{\mathbf{O}}_W$, begins at the current orientation, $\mathbf{O}_W$, and lies on the tangent plane of the sphere denoted here as Π (Figure 3). This vector has a *vertical component*, $\dot{\Theta}_v$, corresponding to an A axis movement and a *horizontal component*, $\dot{\Theta}_h$, corresponding to a

C axis movement where

$$\begin{aligned}\dot{\mathbf{O}}_W &= \frac{\partial \mathbf{O}_W}{\partial t} = \frac{\partial \mathbf{O}_W}{\partial A}\frac{\partial A}{\partial t} + \frac{\partial \mathbf{O}_W}{\partial C}\frac{\partial C}{\partial t} \\ &= \hat{\mathbf{t}}_v\dot{\Theta}_v + \hat{\mathbf{t}}_h\dot{\Theta}_h\end{aligned}$$

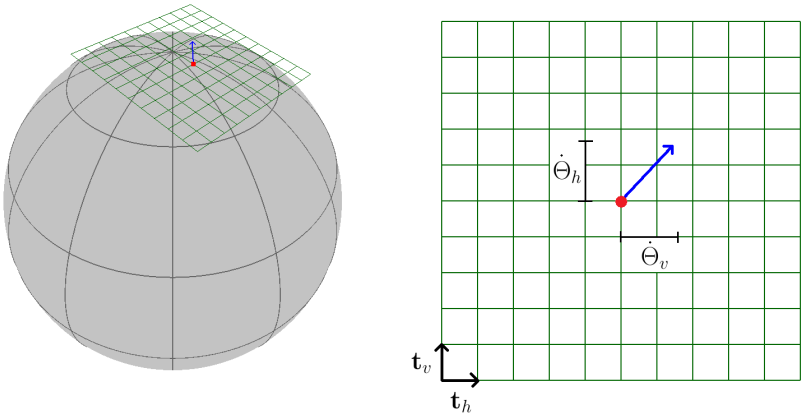

Figure 3: Left: Orientation vector $\mathbf{O}_W$ and the derivative $\dot{\mathbf{O}}_W$. Right: Tangent plane Π used to form the vertical and horizontal components $\dot{\Theta}_v$ and $\dot{\Theta}_h$ of $\dot{\mathbf{O}}_W$.

The vertical component acts in the direction towards the singularity, $(0, 0, 1)^T$, of the sphere and the horizontal component acts orthogonally to this. These directions can be calculated with consideration for the velocity of a point under rotation. From the definition of angular velocity, ω, the following observation is made.

$$\frac{d\mathbf{r}}{dt} = \omega(t) \wedge \mathbf{r} \quad \Rightarrow \quad \frac{\partial}{\partial \phi}\Big(\mathbf{R}_\omega(\phi)\hat{\mathbf{u}}\Big) = \omega \wedge \mathbf{R}_\omega(\phi)\hat{\mathbf{u}}.$$

Therefore

$$\frac{\partial \mathbf{O}_W}{\partial A} = \mathbf{R}_z(C)\frac{\partial \mathbf{R}_x(A)\mathbf{O}_M}{\partial A} = \mathbf{R}_z(C)(\hat{\mathbf{x}} \wedge \mathbf{R}_x(A)\mathbf{O}_M),$$

$$\frac{\partial \mathbf{O}_W}{\partial C} = \frac{\partial \mathbf{R}_z(C)\mathbf{R}_x(A)\mathbf{O}_M}{\partial C} = \hat{\mathbf{z}} \wedge \mathbf{R}_z(C)\mathbf{R}_x(A)\mathbf{O}_M = \hat{\mathbf{z}} \wedge \mathbf{O}_W,$$

and thus

$$\hat{\mathbf{t}}_v = \mathbf{R}_z(C)(\hat{\mathbf{x}} \wedge \mathbf{R}_x(A)\mathbf{O}_M), \quad \hat{\mathbf{t}}_h = \frac{\hat{\mathbf{z}} \wedge \mathbf{O}_W}{||\hat{\mathbf{z}} \wedge \mathbf{O}_W||}.$$

Note that when $A = 0$ then $\mathbf{t}_h = \hat{\mathbf{z}} \wedge \hat{\mathbf{z}} = \mathbf{0}$. This implies that changing the C-axis here does not change the orientation. This demonstrates a (redundant input) machine singularity [4]. This singularity feature will be revisited later but first the amount of contribution to $\dot{\mathbf{O}}_W$ from the A- and C- axes is discussed.

The vertical and horizontal components of $\dot{\mathbf{O}}_W$ are given as

$$\dot{\mathbf{O}}_W = \dot{\Theta}_v \hat{\mathbf{t}}_v + \dot{\Theta}_h \hat{\mathbf{t}}_h \quad \Rightarrow \quad \dot{\Theta}_v = \dot{\mathbf{O}}_W \cdot \hat{\mathbf{t}}_v, \quad \dot{\Theta}_h = \dot{\mathbf{O}}_W \cdot \hat{\mathbf{t}}_h.$$

These components form the vector $\dot{\mathbf{O}}_W$ and thus $|\dot{\mathbf{O}}_W| = \dot{\Theta} = \sqrt{\dot{\Theta}_v^2 + \dot{\Theta}_h^2}$. Furthermore both components are bounded by $\dot{\Theta}$, that is $|\dot{\Theta}_v|, |\dot{\Theta}_h| < \dot{\Theta}$. The two separate components, $\dot{\Theta}_v$ and $\dot{\Theta}_h$, are related to movements in the A- and C- axes respectively as is now discussed.

Consider a tool path with a vertical orientation change with no horizontal change, then $\dot{\mathbf{O}}_W = \lambda \hat{\mathbf{t}}_v$ for some $\lambda \in \mathbb{R}$. This corresponds to a movement in just the A-axis. The change in orientation angle, Θ_v, corresponds to the length of the path traced onto the sphere by $\mathbf{O}_W$. The path traced out forms an arc segment of a unit circle through both poles.

Now consider a tool path with a horizontal orientation change with no vertical change, then $\dot{\mathbf{O}}_W = \mu \hat{\mathbf{t}}_h$ for some $\mu \in \mathbb{R}$. This corresponds to a movement in just the C-axis. The change in orientation angle, Θ_h, corresponds to the length of the path traced onto the sphere by $\mathbf{O}_W$. The path traced out forms an arc segment of a horizontal (latitudinal) circle.

Note that angle changes in longitude, Θ_v, are measured with respect to the unit circle. This means a change in longitude corresponds to the same change in A. Latitudinal differences however are measured from the horizontal circles at $\mathbf{O}_V$. The size of these horizontal circles (circumference size relative to the unit circle) depends upon A and can be shown to equal $\sin(A)$ (Figure 4). Hence the horizontal angle Θ_h is measured with respect to the size of this circle. This property can also be seen from

$$||\frac{\partial \mathbf{O}_W}{\partial C}|| = ||\hat{\mathbf{z}} \wedge \mathbf{O}_W|| = \sin(A).$$

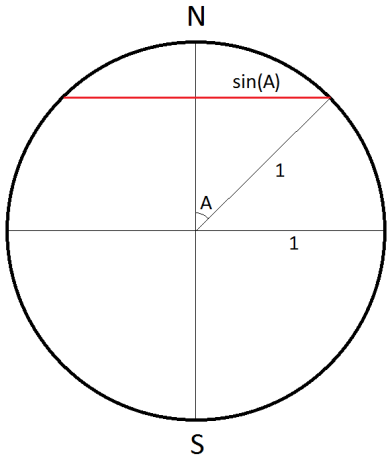

Figure 4: Cross section of the unit sphere. The circumference of the horizontal circles, relative to the unit circle, is $\sin(A)$.

Therefore:

$$\frac{\partial \mathbf{O}_W}{\partial A} = \hat{\mathbf{t}}_v, \quad \frac{\partial \mathbf{O}_W}{\partial C} = \sin(A)\hat{\mathbf{t}}_h.$$

or equivalently

$$\frac{\partial \Theta}{\partial A} = \frac{\partial \Theta_v}{\partial A} = 1, \quad \frac{\partial \Theta}{\partial C} = \frac{\partial \Theta_h}{\partial C} = \sin(A), \tag{3}$$

The amount of movement in the A- and C- axes does not depend solely upon the change of orientation, $\dot{\Theta}$, but rather the horizontal and vertical components. Furthermore the amount of C-axis movement depends upon the A-axis position.

As A approaches zero, movements of the C-axis have diminishing effect, indicative of a redundant input singularity [4]. The effect of near-singular configurations on the rotary AC-axes, as well as the positional XYZ-axes, is described in the following section.

2.3. Movement of machine axes along a tool path

The undesired behaviour of the machine tool local to the singularity manifests itself as a sharp variation in machine axes movements with respect to constant cutting feed rate [2]. In order to identify this abrupt change in speed the relationship of workpiece and machine coordinate systems can be linked via this feed rate. By taking a constant and thus controlled feed rate, unstable machine axes movements can in part be associated to singular behaviour. Let the following equation represent this assumption of constant cutting feed rate:

$$\left|\left|\frac{\partial \mathbf{P}_W}{\partial t}\right|\right| = f, \tag{4}$$

where f represents the cutting feed rate of the tool path and t represents time.

Since the two rotary axes are only affected by orientation changes these are studied first. The movements can be obtained from (3) as:

$$\frac{\partial A}{\partial t} = \frac{\partial A}{\partial \Theta_v}\frac{\partial \Theta_v}{\partial t} = \frac{\partial \Theta_v}{\partial t}, \qquad \frac{\partial C}{\partial t} = \frac{\partial C}{\partial \Theta_h}\frac{\partial \Theta_h}{\partial t} = \frac{1}{\sin(A)}\frac{\partial \Theta_h}{\partial t}. \tag{5}$$

Note that $\frac{\partial \Theta}{\partial t}$ represents the rate of orientation change (as the tool traverses the tool path). It is assumed that the CAM software has generated suitable tool path trajectories and hence this value has been controlled. Therefore the movement of the A-axis should be stable. The movement of the C-axis however is unstable as $\sin(A) \to 0$. Singular behaviour, identified as a large increase in C-axis speed, can occur as $A \to 0$. Interestingly it is only the C-axis movements which are unstable and the stability depends upon the A-axis angle. The singular behaviour of the C-axis also affects the positional axes.

Now consider the movement of the machine's positional axes with respect to constant cutting feed rate. The XYZ-axes correspond to $\mathbf{P}_M$ and are affected by the rotary table angles as per equation (1). Differentiating via the product rule:

$$\begin{aligned}
\frac{\partial \mathbf{P}_M}{\partial t} &= \frac{\partial}{\partial t}\Big(\mathbf{R}_A \mathbf{R}_C \mathbf{P}_W\Big) \\
&= \frac{\partial \mathbf{R}_A}{\partial t}\mathbf{R}_C \mathbf{P}_W + \mathbf{R}_A \frac{\partial \mathbf{R}_C}{\partial t}\mathbf{P}_W + \mathbf{R}_A \mathbf{R}_C \frac{\partial \mathbf{P}_W}{\partial t} \\
&= \frac{\partial}{\partial A}\mathbf{R}_A \mathbf{R}_C \mathbf{P}_W \frac{\partial A}{\partial t} + \frac{\partial}{\partial C}\mathbf{R}_A \mathbf{R}_C \mathbf{P}_W \frac{\partial C}{\partial t} + \mathbf{R}_A \mathbf{R}_C \frac{\partial \mathbf{P}_W}{\partial t} \\
&= \frac{\partial \mathbf{P}_M}{\partial A}\frac{\partial A}{\partial t} + \frac{\partial \mathbf{P}_M}{\partial C}\frac{\partial C}{\partial t} + \mathbf{R}_A \mathbf{R}_C \frac{\partial \mathbf{P}_W}{\partial t} \qquad (6)
\end{aligned}$$

where $\mathbf{R}_A = \mathbf{R}_x(-A)$ and $\mathbf{R}_C = \mathbf{R}_z(-C)$.

The first term, $\frac{\partial \mathbf{P}_M}{\partial A}\frac{\partial A}{\partial t}$, describes how the machine compensates for the changing A-axis. This requires following a circle, traced out by (X, Y, Z) as it rotates about the A-axis. Similarly the second term, $\frac{\partial \mathbf{P}_M}{\partial C}\frac{\partial C}{\partial t}$, describes the

machine compensating for the changing C-axis. This again requires following a circle, this time traced out by (X, Y, Z) as it rotates about the C-axis. The third term, $\mathbf{R}_A\mathbf{R}_C\frac{\partial \mathbf{P}_W}{\partial t}$, corresponds to cutting feed (rotated through the origin but of the same magnitude).

Near to a singularity, it was shown that the C-axis is required to rotate at large speeds to maintain a given cutting feed. This was a result of a diminishing effect of the C-axis on the orientation of the cutter by equation (5). This means that the second term can be become unbounded (by $1/\sin(A)$) and consequently when the machine compensates for the rapidly moving C-axis, the (X, Y, Z) positional axes follow, resulting in the observable undesired machine axes behaviour. Thus it appears as though all the undesirable singular behaviour is caused by the secondary rotary axis movements. This characteristic is not unique to the Hermle C600U. A similar singularity analysis can be deduced for an arbitrary machine tool configuration.

2.4. Singularities of general five-axis machine tool configurations

A general machine axis configuration consists of three translational axes (T_1, T_2, T_3) and two rotary (R_1, R_2) axes. The translational axes do not affect the orientation vector $\mathbf{O}_W$. This (unit) vector depends only upon the rotary axes and therefore shares a similar form to Equation (2):

$$\mathbf{O}_W = \mathbf{R}_{\mathbf{r}_2}(R_2)\mathbf{R}_{\mathbf{r}_1}(R_1)\mathbf{O}_M$$

where $\mathbf{r}_1$ and $\mathbf{r}_2$ are the axes of rotation for the rotary axes R_1 and R_2 respectively and O_M is the orientation of the cutter with respect to the machine. The effect of changing each axis on the orientation is similarly

characterised by two tangent vectors from the tangent plane:

$$\mathbf{t}_{R_1} = \frac{\partial \mathbf{O}_W}{\partial R_1} = \mathbf{R}_{\mathbf{r}_2}(R_2)\frac{\partial \mathbf{R}_{\mathbf{r}_1}(R_1)\mathbf{O}_M}{\partial R_1} = \mathbf{R}_{\mathbf{r}_2}(R_2)(\mathbf{r}_1 \wedge \mathbf{R}_{\mathbf{r}_1}(R_1)\mathbf{O}_M)$$

$$\mathbf{t}_{R_2} = \frac{\partial \mathbf{O}_W}{\partial R_2} = \frac{\partial \mathbf{R}_{\mathbf{r}_2}(R_2)\mathbf{R}_{\mathbf{r}_1}(R_1)\mathbf{O}_M}{\partial R_2} = \mathbf{r}_2 \wedge \mathbf{R}_{\mathbf{r}_2}(R_2)\mathbf{R}_{\mathbf{r}_1}(R_1)\mathbf{O}_M = \mathbf{r}_2 \wedge \mathbf{O}_W$$

A singularity is immediately observed at $\mathbf{O}_W = \mathbf{r}_2$ since this implies $\mathbf{t}_{R_2} = \mathbf{0}$. Furthermore, this shows that every five-axis machine tool has a singular configuration when the orientation of the cutter is aligned with axis of rotation of the secondary rotary axis.

3. Singularity Avoidance Strategy

This section proposes an approach to singularity avoidance by reorientation of the workpiece. Drawbacks of existing techniques are discussed which motivate the new approach. The effect of reorientation on machine tool paths is explained leading to a simple procedure for singularity avoidance. Possible issues with reorientation are then discussed and solutions presented.

3.1. Drawbacks of current strategies

Most singularity avoidance procedures include a manipulation strategy to locally adjust any tool paths in the CAM stage that are close to a singularity. This is achieved by reorienting the cutter within affected regions. This local adjustment raises concerns for the overall machining strategy as discussed below.

Firstly, the tool has to be reoriented such that the cutter contact (CC) point (where the cutter contacts material) is preserved. This results in a new cutter location (CL) point, i.e. new machine coordinates, which may

result in gouging or collisions. Furthermore, the ability to reorient the tool and maintain the CC point depends upon the geometry of the tool. For example, ball end mills can be reoriented with relative simplicity. Flat end mills and small radius tipped tools on the other hand cannot accommodate large alterations to cutter orientations [8]. Flank milling strategies are not compatible with a reorientation since the side of the tool has to be flush with the surface of the CAD model.

Another drawback of local alteration to cutter orientation is the effect on the surface finish of the material. Machining strategies in CAM often try to preserve the orientation of the cutter with respect to the surface normal and feed direction. The angle between the axis of the cutter and surface normal is the tilt angle. The angle between the direction of motion and the axis of the cutter is the yaw angle. Adjustment of cutter orientation affects both tilt and yaw angles. This in turn affects the chip pattern on the surface of the material [11]. If adjustments are made locally around a singularity, there may be a visible change in the texture of the finished surface [5]. Such changes are undesirable and ideally should be avoided.

Local adjustments to the cutter orientations can be avoided by instead using a global adjustment procedure. Rather than reorienting the cutter with respect to the workpiece it is possible to reorient the workpiece with respect to the machine. This can be achieved through the use of a jig. The CAM tool path needs to be correspondingly reoriented but there is no need to regenerate the tool paths.

3.2. Reorientation of the workpiece

The idea of reorienting the workpiece with respect to the machine is used in Makhonov [12]. This approach uses the degrees of freedom associated with reorientation of the workpiece in an optimisation function to increase geometric accuracy. It is claimed that changing the initial set-up is a "*very simple, zero cost operation*" and thus a feasible approach. The proposed reorientation of the workpiece is now outlined.

The workpiece is mounted on a jig which allows it to tilt about a horizontal axis which is taken as a local x-axis. The rotation angle is θ_x. In addition the workpiece can rotate about the axis perpendicular to the plane of the jig. This is the local z-axis. The rotation angle is θ_z. The following kinematic chain describes the link between orientations of the cutter with respect to the workpiece without the jig, $\mathbf{O}_W$, and with the jig, $\overline{\mathbf{O}_W}$, (Figure 5).

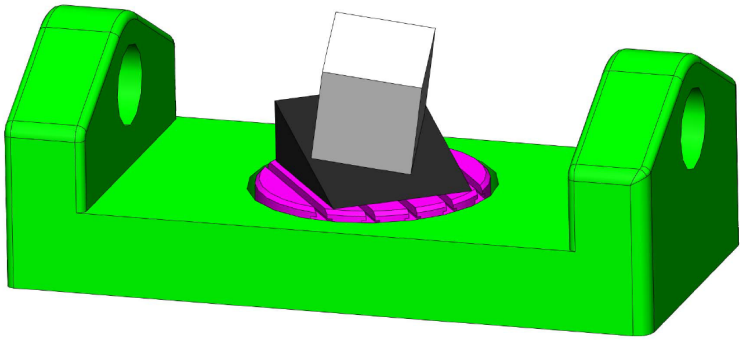

Figure 5: Reorienting the workpiece (white) via the use of a jig (black).

$$\overline{\mathbf{O}_W} = \mathbf{R}_x(\theta_x)\mathbf{R}_z(\theta_z)\mathbf{O}_W. \tag{7}$$

Singularities of the modified tool path occur when the reoriented cutter is perpendicular to the machine bed. The orientation, $\mathbf{S}$, in workpiece

coordinates can be deduced from the kinematic chain of (7).

$$\mathbf{R}_x(\theta_x)\mathbf{R}_z(\theta_z)\mathbf{S} = (0,0,1)^T.$$

The orientation of the singularity in the original tool path thus corresponds to the vector:

$$\mathbf{S} = \mathbf{R}_z(-\theta_z)\mathbf{R}_x(-\theta_x)(0,0,1)^T.$$

This reorientation procedure has had the effect of changing the singularity for the original tool path. Furthermore, by altering the angles θ_x and θ_z the singularity can be oriented with respect to the workpiece in an arbitrary direction (Table 1 of Section 2.1 can be used to find θ_x and θ_z). There is thus choice for the reorientation and scope for finding optimal values.

This low-cost solution also has the benefit of flexibility. Reorientation configurations can be deduced for a variety of different motivations. An optimisation of some cost function, similar to that of [12], can be employed. Alternatively, control over the reorientation can be given to human machine operators who independently decide what is best to suit their purpose.

3.3. Potential concerns with reorientation approach

A fundamental restriction depends upon the swivelling range of the A-rotary axis. For the Hermle C600U this angle must be between $\pm 110°$. Tool paths in the new system must not go outside this range otherwise their machining would not be physically possible. This needs to be considered when determining the suitability of a reorientation.

Gouges and collisions with the workpiece are not a concern since the tool paths relative to the workpiece do not change. Another concern is that

with the new orientation collisions of the spindle with the rotary bed and jig may now occur. Many CAM software packages provide checks for machine collisions. The only overhead required is thus creating the jig in the software and checking for collisions. If collisions do occur then a strategy of moving the workpiece with respect to the top surface of the jig and the jig with respect to machine bed should be employed. If this repositioning strategy is unsuccessful then a different orientation must be considered. One such approach may be to decrease θ_x which rotates the tool paths closer to the original orientation. It may not always be possible to avoid singular regions altogether but the added flexibility allows other motivations to be considered, such as ensuring singular behaviour is confined to less critical regions on the component.

3.4. Extension to different machine configurations

The derivations presented may appear to be based on the kinematic chain for the Hermle C600U but this reorientation strategy may be applied to general machine axis configurations. It can be reasoned that reorienting the workpiece with respect to the machine bed (with the use of a jig) has an equivalent effect regardless of machine configuration.

The effect of reorientation on the workpiece has a simple intuitive interpretation. Tool path orientations can be visualised by mapping them onto the unit sphere. The reorientation strategy has the effect of rotating this sphere with respect to the original whilst preserving the direction of the singularity. One can interpret this equivalently as reorientation of the workpiece preserves the orientation vectors (with respect to the workpiece) but relocates the singularity on the sphere. The only difference between machine

configurations is the location of the singularity on the sphere. Furthermore the same reorientation strategy of Section 3.2 can be applied to any five-axis machine tool.

4. Machining Example

In this section the effectiveness of the reorientation procedure is investigated with machining experiments. To begin a relatively simple tool path is constructed that is expected to experience singular behaviour. The singular behaviour is confined to a specific region of the part and after machining this region is inspected for defects. A second tool path is then developed which is a reorientation of the first. After machining, the same region is compared to the first experiment.

The machining strategy of flank milling is chosen to provide significant area on the part for examination of the surface finish. The material chosen for machining is a $50 \times 50 \times 50\ mm^3$ block of aluminium. Aluminium is chosen because an expected consequence of machining near to a singular configuration is a slow down in cutting feed, to accommodate excessive machine axis kinematics, and thus a potential for rubbing of the cutter. Aluminium has a propensity to melt under rubbing [13] (due to its high thermal expansion coefficient) and thus may exhibit an indicator for such behaviour in the form of a surface defect.

The tool tip ($\mathbf{P}_W$) is made to move in a straight line across the face of the aluminium block. The orientation, $\mathbf{O}_W$, is constructed to have constant orientation speed, $\dot{\Theta}$. A simple construction for this constraint is a semi-circular path on the unit sphere. Circles of small radius have excessive

orientation speed and limited angle range. Circles with large radius have slow orientation speed and excessive angle range. To reduce the range of the A-axis, and thus eliminate the need for special holding jigs, and maintain a suitable orientation speed, a radius of $\sin(10^\circ)$ is chosen. Singular behaviour is expected when the angle between the orientation vector and the singular configuration ($\mathbf{O}_W = (0, 0, 1)^T$) is small and $\mathbf{O}_W$ lies within a singular region. The size of this region is chosen here as 1° which is predicted to exhibit singular behaviour.

The first tool path is constructed such that its zenith (orientation closest to singularity) is reached halfway along the tool path at an angle of 1°. A graphical representation of this tool path is given in Figure 6 which also illustrates the orientation of the cutter as well as a simulation for the expected shape of the part after cutting.

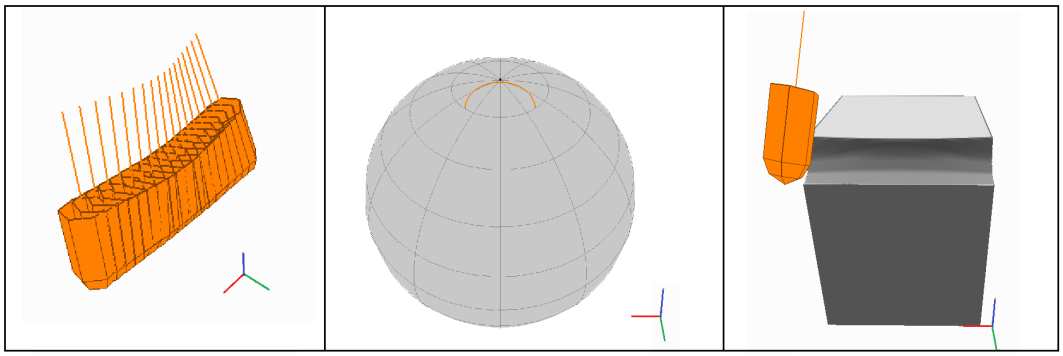

Figure 6: [Left] Visualisation of the linear tool path. [Center] The tool orientations ($\mathbf{O}_W$) visualized on the unit sphere. [Right] Simulated part shape after machining.

A workpiece coordinate origin is located at the top-front-left vertex of the $50 \times 50 \times 50$ mm^3 cube. This establishes a datum for the NC code and can be calibrated with the machine tool using an edge-finding procedure. A

value of $h = 8mm$ is used to represent the depth of cut. This is chosen to provide a significant amount of machined area for inspection. A value of δ_s is used to control the step-over for sequential tool path passes. This is chosen as 0.5mm in the roughing stage until a depth of 5mm is achieved. Then a 0.2mm step-over is used in a finishing pass. The type of cutter is chosen to be a 10mm ball-nose steel end mill for use with a lubricating coolant. A feed rate of 2000mm/min and spindle speed of 12,000 rpm is chosen based on preliminary tests. The formulation of the tool path is now given in the following equation.

$$\mathbf{P}_W(t) = \begin{pmatrix} x \\ y \\ z \end{pmatrix} = \begin{pmatrix} \frac{100}{3}t \\ \delta_s \\ -h \end{pmatrix}, \quad t \in [0, \tfrac{3}{2}] \tag{8}$$

$$\mathbf{O}_W(t) = \mathbf{R}_x(11^\circ)\mathbf{R}_z(120^\circ t)\mathbf{R}_x(-10^\circ)\hat{\mathbf{z}}, \quad t \in [0, \tfrac{3}{2}] \tag{9}$$

From the workpiece coordinates the machine coordinates of the tool path can be calculated by applying the inverse kinematics as outlined in section 2.1. Any singular behaviour of the rotary axes will cause singular behaviour in the positional axes (as per Equation 6). Furthermore the positional axes (XYZ) depend upon the location of the datum. The rotary axes on the other hand do not. Therefore the machine kinematics of the rotary axes only are considered for analysis (Figure 7).

Halfway through the tool path it is noted that the C-axis is required to spin at a maximum speed of around 200 rpm (Figure 7). However the maximum speed of the rotary axes for the Hermle C600U is around 25 rpm, as

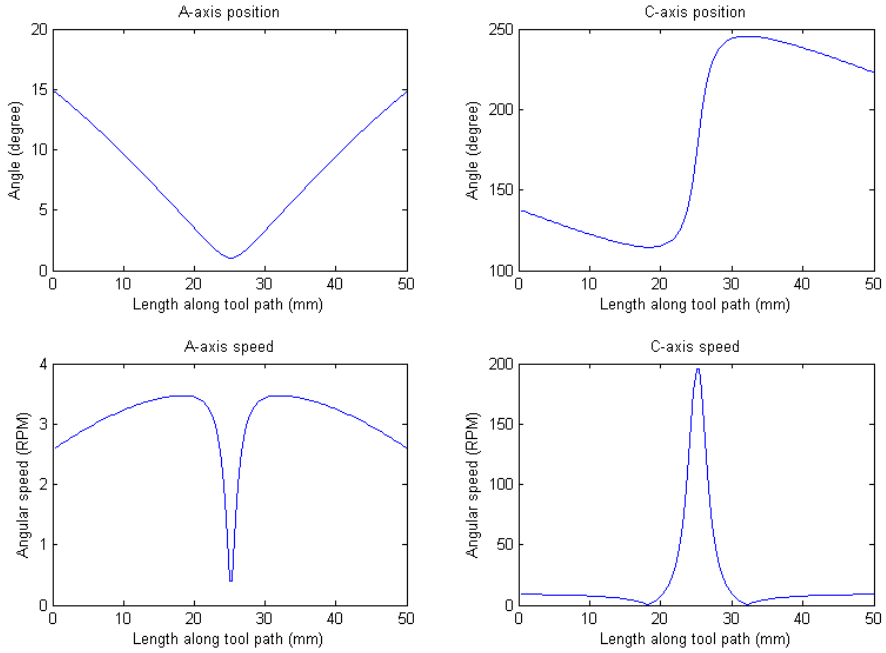

Figure 7: Kinematics of the rotary axes with a feed rate 2000mm/min. [Left] A-axis [Right] C-axis [Top] Axis angle [Bottom] Axis speed.

stated by the machine tool manufacturers [9]. Therefore the CNC controller has to make a compromise on the desired tool path motion. The predicted compromise is a reduction in cutting feed rate. Low feed rates, with high spindle speeds, cause rubbing of the tool on the material. This can cause aluminium to melt and hence there is a potential for surface defects during the regions with excessive rotary axis speeds. This occurs between 23-27mm across the part.

The next step is to formulate the NC-codes for use with the Hermle C600U machine tool. G-code files were written for use with the CNC controller based upon the desired tool path motion in Equations (8) and (9). An edge-finding

procedure was used to obtain the location of the top-front-left vertex of the $50 \times 50 \times 50\ mm^3$ cube. This acts as a datum for the tool path and the step-over is controlled by iterating the y-coordinate of this datum. The actual G-code used can be found in Appendix 1.

After machining the part it was inspected with the Alicona G5 Infinite-Focus, a 3D micro coordinate measurement machine and surface roughness measurement device [14]. The images taken (Figure 8) illustrate the presence of a surface defect in the form of a discolouration of the material at the center of the part. Furthermore, a roughness profile measurement taken across the part ($z = -3mm, x = 2 \ldots 3mm$) indicates an increase in surface roughness local to the predicted affected region of between 23-27mm across the part (Figure 9). The surface defect is thought to be melting of the aluminium and a consequence of singular behaviour.

It was proposed, in section 3.2, that singularities can be avoided by re-orienting the workpiece. The tool path should then be correspondingly re-orientated. A second tool path, based upon the previous tool path, is to be constructed in such a way. However, for ease of set-up, the workpiece is not actually reoriented with the use of a jig. This will cause a different shape to be machined but nonetheless share similar machining conditions.

The second tool path is chosen to be reoriented by 10° in the direction away from the singularity (so its zenith will be 11° away). This is predicted to be of a significant enough angle to eliminate singular behaviour but not too large to require special holding jigs. The formulation of the second tool path is given in the following equations (10) and (11).

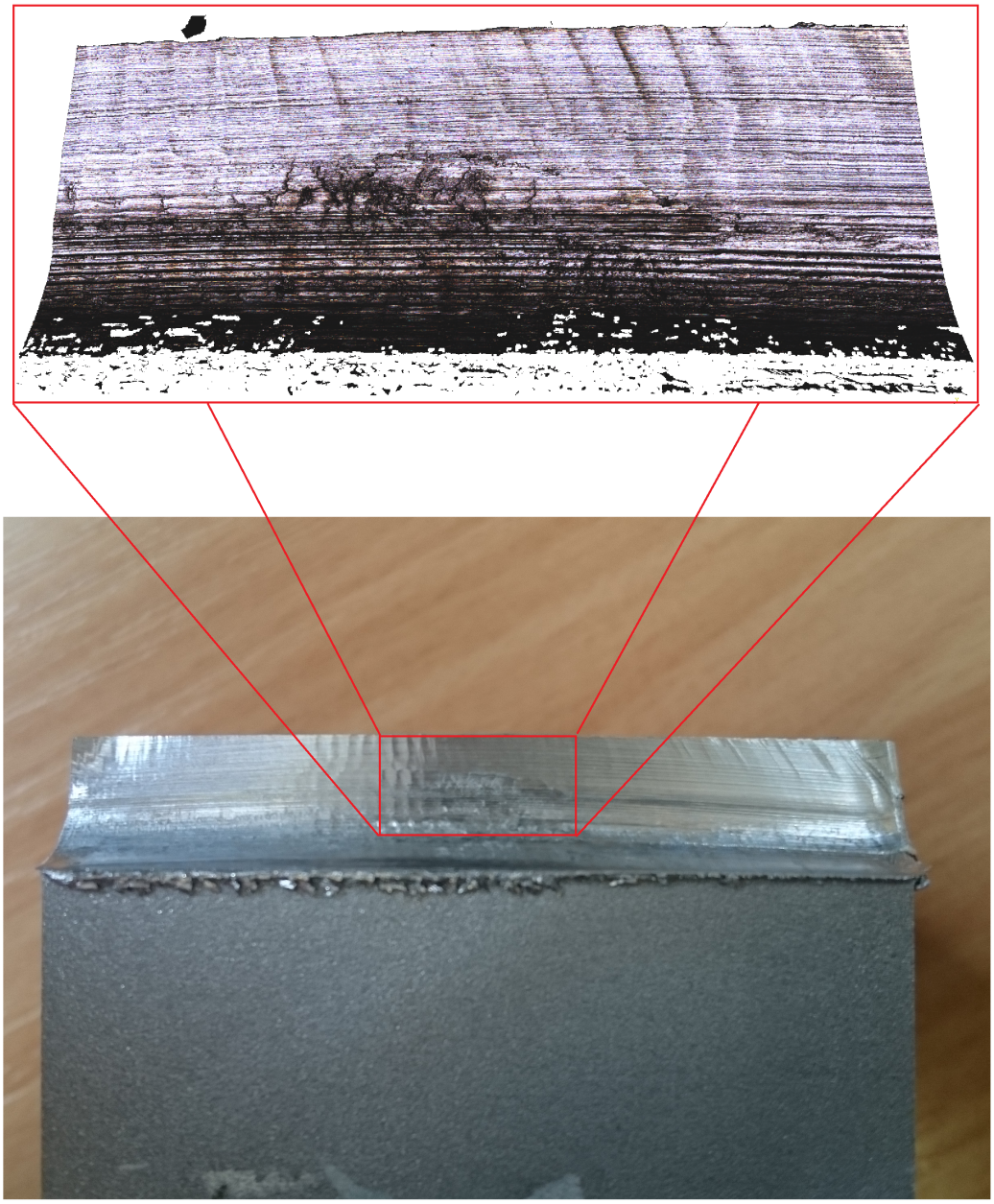

Figure 8: Image showing surface defect occurring near to singularity.

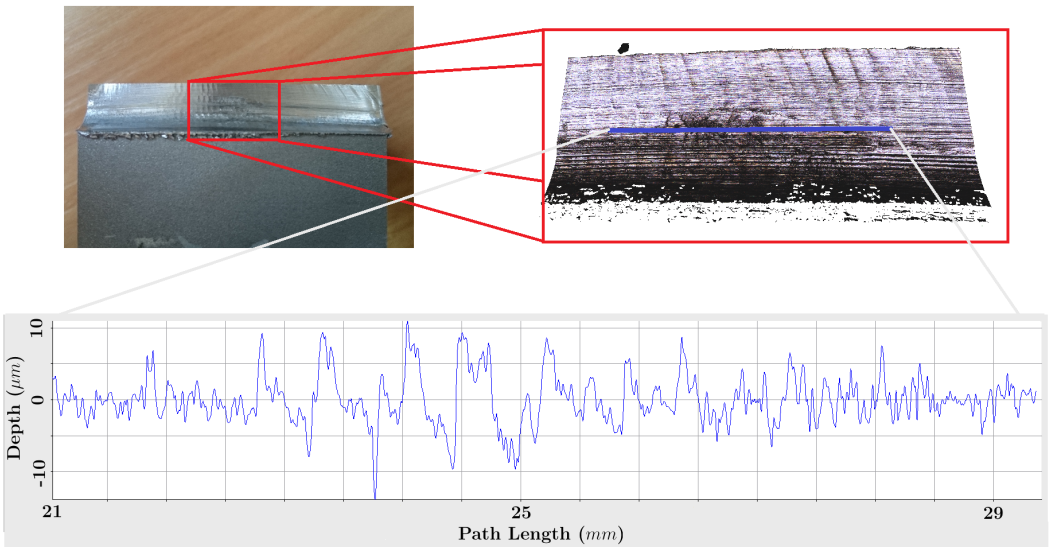

Figure 9: Surface roughness profile of the machined surface.

$$\mathbf{P}_W(t) = \begin{pmatrix} x \\ y \\ z \end{pmatrix} = \begin{pmatrix} \frac{100}{3}t \\ \delta_s \\ -h \end{pmatrix}, \quad t \in [0, \tfrac{3}{2}] \tag{10}$$

$$\mathbf{O}_W(t) = \mathbf{R}_x(21^\circ)\mathbf{R}_z(120^\circ t)\mathbf{R}_x(-10^\circ)\hat{\mathbf{z}}, \quad t \in [0, \tfrac{3}{2}] \tag{11}$$

The corresponding G-code can be found in Appendix 2. A graphical representation of this tool path is given in Figure 10 which also illustrates the orientation of the cutter as well as a simulation for the expected shape of the part after cutting.

Applying the inverse kinematics to the second tool path generates the machine coordinates. Focusing on the rotary axes a reduction in the maximum

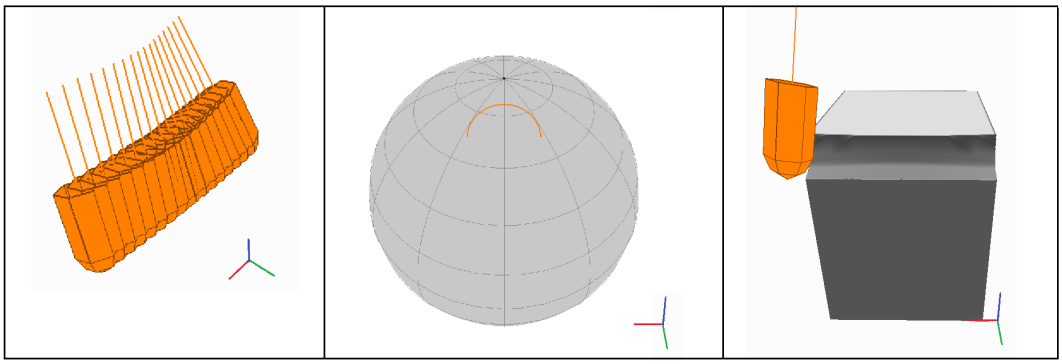

Figure 10: [Left] Visualisation of the second tool path. [Center] The modified tool orientations ($\mathbf{O}_W$) visualized on the unit sphere. [Right] Simulated part shape after machining.

speed of the C-axis is observed (Figure 11). Applying the reorientation has had the effect of reducing this value from around 200 rpm to around 18 rpm. This value is below the C-axis maximum speed and is therefore not expected to cause the same issues as in the first tool path. Recall that with excessive rotary axis speed a reduction in cutting feed and increase in tool rubbing was predicted. Therefore an improvement in surface finish is expected.

After machining, the part was again inspected with the Alicona InfiniteFocus. The image in Figure 12 confirms that the surface defect from the original tool path, explained as a consequence of singular behaviour, has been successfully removed through reorientation.

4.1. Further comments on machining tests

Perhaps the most striking distinction between the tool paths is the dynamics of the machine tool. This is an immediate consequence of traversing near to a singularity. Secondary effects, such as producing surface defects, are a consequence of this behaviour. Ideally the dynamics/kinematics of the

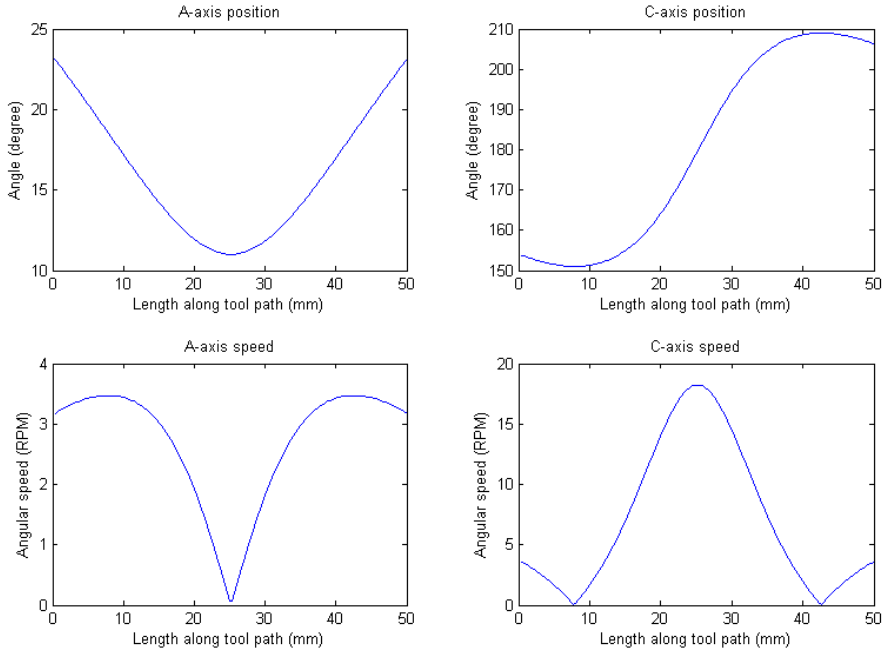

Figure 11: Kinematics of the rotary axes (reorientated tool path) with a feed rate 2000mm/min. [Left] A-axis [Right] C-axis [Top] Axis angle [Bottom] Axis speed.

axes would have been measured in these experiments but unfortunately this was not possible. There are however video recordings of the different tool paths which contrast the dynamics between them (available online). In particular the footage (with audio) demonstrates the machine tool *stuttering* through the singularity affected region as predicted.

It is worth recognising that a significant effort had to be spent in creating the secondary effect (surface defect) from the primary effect (undesirable kinematics). For example, using a carbide cutter instead of the steel cutter removed any singular features. Changing the spindle/feed rate caused different surface defects, such as from chattering, to dominate any singularity

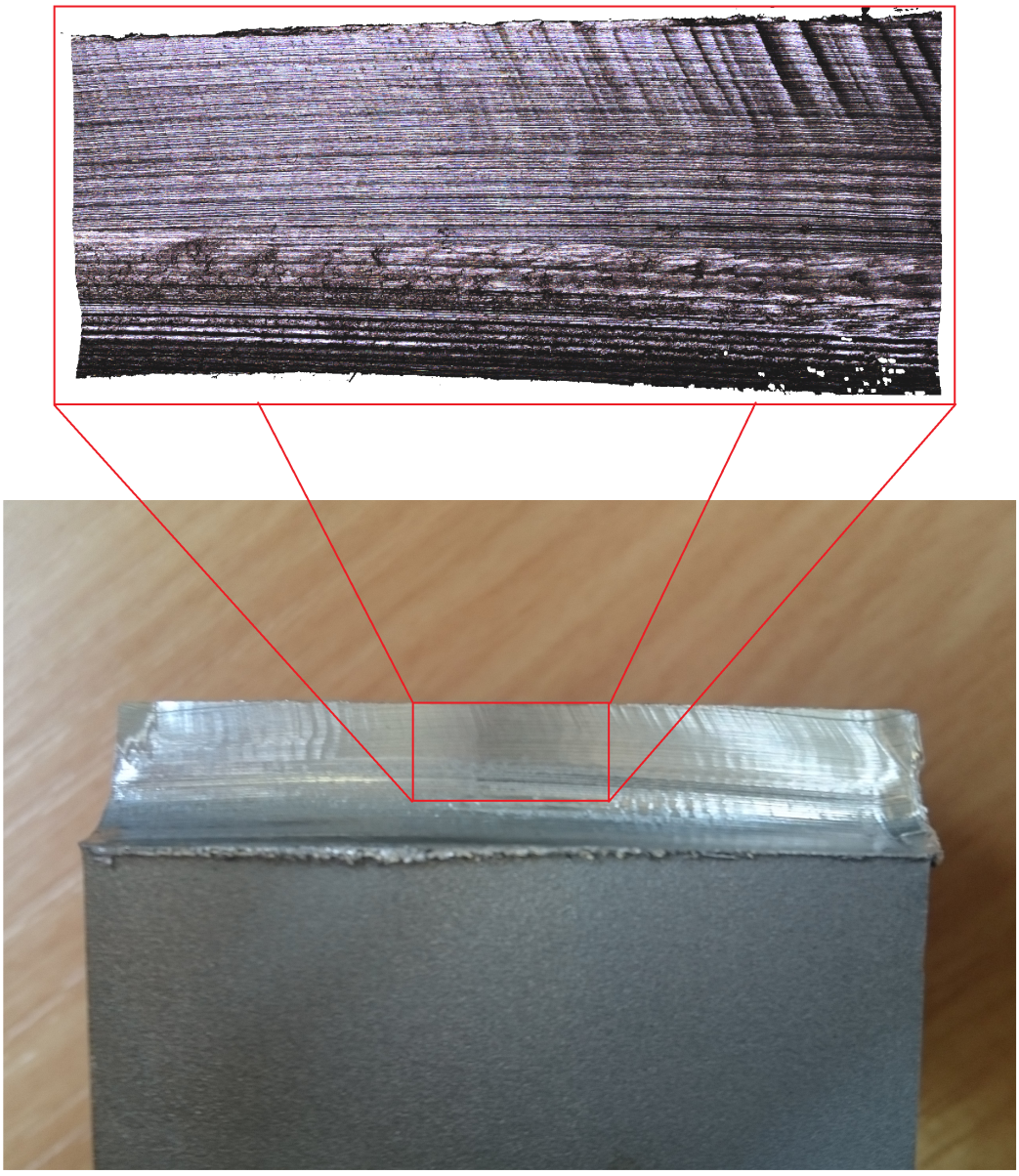

Figure 12: Image showing removal of surface defect (compared to Figure 8).

feature. Part of this difficulty can be attributed to the robustness of the CNC controller. It also emphasises a hierarchical importance of factors in-

volved with machining: choosing the appropriate machining parameters is paramount. However, as the demand for tolerances on surface finish improve over time, better control of cutting conditions will be required. For this reason it will become more essential to avoid singular behaviour.

5. Conclusions

Singular behaviour of machine tools has long been observed at certain cutter orientations. This manifests itself as a sharp variation in machine axes movements at constant cutting feed rate. This motivated the identification of a link between machine axes movements and the cutting feed rates. Two separate coordinate systems were used to obtain equations to model this link. From the equation describing machine axes movements (5) singular behaviour was associated with a divergent $1/\sin(A)$ term. This associated the undesired machine behaviour to the singular configurations and in effect explains its cause.

A new approach is proposed to avoid singular regions. Drawbacks of existing strategies are caused by local manipulations of cutter orientations, which include collision and surface finishing concerns. The approach presented here involved reorienting the workpiece with the use of a jig. This means that the original orientations of the cutter with respect to the workpiece are preserved, maintaining consistency with the original tool paths. Furthermore, the effect of this reorientation on the workpiece has a simple intuitive interpretation. To begin, tool path orientations are visualised by mapping them onto the unit sphere. The reorientation strategy has the effect of rotating this sphere. This means that the singularity can be placed anywhere on the sphere by

finding the corresponding configuration of θ_x and θ_z (Section 3.2).

Machining experiments demonstrated the cause, effect and avoidance of singularities. The "*cause*" of singular features, undesirable machine axis kinematics, was observed in the original tool path. The "*effect*" of singularities, surface defects, was then discovered in the predicted region. Finally "*avoidance*" of singular features, by reorientation, was achieved with the modified tool path.

An interesting consequence of the equation describing machine axes movement (5) is not purely the existence of the singularity. The effect of the *closeness* to the singularity is quantified by the $1/\sin(A)$ term. This raises a question of *how close to the singularity should the tool path get*? Current arguments are based on machine tolerances to establish a singular region. For example, the values in [6] and [7] require $\phi > 0.00278^\circ$ and $\phi > 0.00573^\circ$ respectively. These correspond to an increase in speed by a factor $1/\sin(A)$ which are greater than $20,000$ and $10,000$ respectively. However, equation (5) suggest that this assertion has no link to the underlying cause. Furthermore the machining experiment in Section 4 demonstrated singular behaviour at $\phi = 1^\circ$. Perhaps a more appropriate approach to singular region definition would be to quantify the effect on machine axes movements. Relating these to bounds on speed/acceleration/jerk would result in a more suitable definition for different machine tools.

Acknowledgement

The research is supported by the EPSRC research council (EP/L010321/1 and EP/L006316/1). The authors would also like to thank Delcam PLC for

supporting the research presented in this paper.

References

[1] W. Zhang, Y.F. Zhang and Q.J. Ge, *Interference-free tool path generation for 5-axis sculptured surface machining using rational Bézier motions of a flat-end cutter*, International Journal of Production Research 43, (2005), p4103-4124.

[2] K. Sørby, *Inverse kinematics of five-axis machines near singular configurations*, International Journal of Machine Tools & Manufacture 47, (2007), p299-306.

[3] X. Beudaert, S. Lavernhe and C. Tournier, *Feedrate interpolation with axis jerk constraints on 5-axis NURBS and G1 toolpath*, International Journal of Machine Tools & Manufacture 57, (2012), p73-82.

[4] D. Zlatanov, R.G. Fenton, B. Benhabib, *Singularity analysis of mechanisms and robots via a velocity-equation model of the instantaneous kinematics*, IEEE International Conference on Robotics and Automation, (1994).

[5] Z. Lin, J. Fu, H. Shen and W. Gan, *Non-singular tool path planning by translating tool orientations in C-space*, International Journal of Advanced Manufacturing Technology 71, (2014), p1835-1848.

[6] A. Affouard, E. Duc, C. Lartigue, J.-M. Langeron and P. Bourdet, *Avoiding 5-axis singularities using tool path deformation*, International Journal of Machine Tools & Manufacture 44, (2004), p415-425.

[7] J. Yang and Y. Altintas, *Generalized kinematics of five-axis serial machines with non-singular tool path generation*, International Journal of Machine Tools & Manufacture 75, (2013), p119-132.

[8] C. Castagnetti, E. Duc and P. Ray, *The Domain of Admissible Orientation concept: A new method for five-axis tool path optimisation*, Computer-Aided Design 40, (2008), p938-950.

[9] Hermle, *Hermle C600 series brochure*, Hermle, Gosheim, Germany, (1999).

[10] D. Kincaid and W. Cheney, *Numerical Analysis*, Second Edition, Brooks/Cole Publishing Company, (1996).

[11] S. Lavernhe, Y. Quinsat and C. Lartigue, *Model for the prediction of 3D surface topography in 5-axis milling*, International Journal of Advanced Manufacturing Technology 51, (2010), p915-924.

[12] S. Makhanov, *Optimization and correction of the tool path of the five-axis milling machine Part 2: Rotations and setup*, Mathematics and Computers in Simulation 75, (2007), p231-250.

[13] S. Kalpakjian, S. Schmid, *Manufacturing Engineering and Technology*, Fifth Edition, Pearson Publishing Company, (2006).

[14] *Alicona G5 InfiniteFocus* Alicona Imaging GmbH, (http://www.alicona.com/products/infinitefocus/ - Accessed August 2016)

Appendix 1: G-code for original tool path.

```
%NON_SING G71 *
N10 G90 *
N20 T5 *
N30 G01 Z+100 F2000 *
N33 X+0 Y+0 *
N36 A+0 C+0 *
N40 M00 *
N50 S12000 M13 *
% DATUM INPUT
N60 G54 X-30.489 Y-4.3 Z+38.054 *
N65 M128 *
N70 G01 X+50 Y+50 Z+100 F2000 *
N80 X+50 Y+50 Z+100 A+23.162 C+333.802 *
N90 X+50 Y+70 Z+100 A+23.162 C+333.802 *
N100 X+50 Y+70 Z-8 A+23.162 C+333.802 *
N110 X+50 Y+50 Z-8 A+23.162 C+333.802 *
N120 X+49 Y+50 Z-8 A+22.586 C+333.177 *
N130 X+48 Y+50 Z-8 A+21.998 C+332.617 *
N140 X+47 Y+50 Z-8 A+21.4 C+332.129 *
N150 X+46 Y+50 Z-8 A+20.792 C+331.718 *
N160 X+45 Y+50 Z-8 A+20.178 C+331.394 *
N170 X+44 Y+50 Z-8 A+19.558 C+331.164 *
N180 X+43 Y+50 Z-8 A+18.934 C+331.038 *
N190 X+42 Y+50 Z-8 A+18.309 C+331.027 *
N200 X+41 Y+50 Z-8 A+17.685 C+331.142 *
N210 X+40 Y+50 Z-8 A+17.064 C+331.397 *
N220 X+39 Y+50 Z-8 A+16.451 C+331.805 *
N230 X+38 Y+50 Z-8 A+15.847 C+332.382 *
N240 X+37 Y+50 Z-8 A+15.256 C+333.143 *
N250 X+36 Y+50 Z-8 A+14.682 C+334.106 *
N260 X+35 Y+50 Z-8 A+14.13 C+335.286 *
N270 X+34 Y+50 Z-8 A+13.605 C+336.7 *
N280 X+33 Y+50 Z-8 A+13.112 C+338.36 *
N290 X+32 Y+50 Z-8 A+12.656 C+340.277 *
N300 X+31 Y+50 Z-8 A+12.243 C+342.455 *
N310 X+30 Y+50 Z-8 A+11.88 C+344.891 *
N320 X+29 Y+50 Z-8 A+11.572 C+347.569 *
N330 X+28 Y+50 Z-8 A+11.326 C+350.463 *
N340 X+27 Y+50 Z-8 A+11.146 C+353.536 *
N350 X+26 Y+50 Z-8 A+11.037 C+356.735 *
N360 X+25 Y+50 Z-8 A+11 C+360 *
N370 X+24 Y+50 Z-8 A+11.037 C+363.265 *
N380 X+23 Y+50 Z-8 A+11.146 C+366.464 *
N390 X+22 Y+50 Z-8 A+11.326 C+369.537 *
N400 X+21 Y+50 Z-8 A+11.572 C+372.431 *
N410 X+20 Y+50 Z-8 A+11.88 C+375.109 *
N420 X+19 Y+50 Z-8 A+12.243 C+377.545 *
N430 X+18 Y+50 Z-8 A+12.656 C+379.723 *
N440 X+17 Y+50 Z-8 A+13.112 C+381.64 *
N450 X+16 Y+50 Z-8 A+13.605 C+383.3 *
N460 X+15 Y+50 Z-8 A+14.13 C+384.714 *
N470 X+14 Y+50 Z-8 A+14.682 C+385.894 *
N480 X+13 Y+50 Z-8 A+15.256 C+386.857 *
N490 X+12 Y+50 Z-8 A+15.847 C+387.618 *
N500 X+11 Y+50 Z-8 A+16.451 C+388.195 *
N510 X+10 Y+50 Z-8 A+17.064 C+388.603 *
N520 X+9 Y+50 Z-8 A+17.685 C+388.858 *
N530 X+8 Y+50 Z-8 A+18.309 C+388.973 *
N540 X+7 Y+50 Z-8 A+18.934 C+388.962 *
N550 X+6 Y+50 Z-8 A+19.558 C+388.836 *
N560 X+5 Y+50 Z-8 A+20.178 C+388.606 *
N570 X+4 Y+50 Z-8 A+20.792 C+388.282 *
N580 X+3 Y+50 Z-8 A+21.4 C+387.871 *
N590 X+2 Y+50 Z-8 A+21.998 C+387.383 *
N600 X+1 Y+50 Z-8 A+22.586 C+386.823 *
N610 X+0 Y+50 Z-8 A+23.162 C+386.198 *
N620 X+0 Y+70 Z-8 A+23.162 C+386.198 *
N630 M00 *
N640 M129 *
N650 G01 Z+150 *
N660 A+0 C+0 *
N670 X+0 Y+0 *
N680 M05 M09*
N690 G54 X+0 Y+0 Z+0 *
N700 G01 X+0 Y+0 Z+150 *
N710 M30 *
N999999 %NON_SING G71 *
```

Appendix 2: G-code for reoriented tool path.

```
%SING G71 *
N10 G90 *
N20 T5 *
N30 G01 Z+100 F2000 *
N33 X+0 Y+0 *
N36 A+0 C+0 *
N40 M00 *
N50 S12000 M13 *
% DATUM INPUT
N60 G54 X-30.489 Y-7.1 Z+38.054 *
N65 M128 *
N70 G01 X+0 Y+0 Z+100 F2000 *
N80 X+0 Y+0 Z+100 A+14.825 C+137.259 *
N90 X+0 Y-20 Z+100 A+14.825 C+137.259 *
N100 X+0 Y-20 Z-8 A+14.825 C+137.259 *
N110 X+0 Y+0 Z-8 A+14.825 C+137.259 *
N120 X+1 Y+0 Z-8 A+14.351 C+135.638 *
N130 X+2 Y+0 Z-8 A+13.864 C+134.031 *
N140 X+3 Y+0 Z-8 A+13.364 C+132.439 *
N150 X+4 Y+0 Z-8 A+12.85 C+130.866 *
N160 X+5 Y+0 Z-8 A+12.325 C+129.313 *
N170 X+6 Y+0 Z-8 A+11.788 C+127.783 *
N180 X+7 Y+0 Z-8 A+11.239 C+126.28 *
N190 X+8 Y+0 Z-8 A+10.68 C+124.808 *
N200 X+9 Y+0 Z-8 A+10.112 C+123.372 *
N210 X+10 Y+0 Z-8 A+9.533 C+121.98 *
N220 X+11 Y+0 Z-8 A+8.946 C+120.641 *
N230 X+12 Y+0 Z-8 A+8.352 C+119.365 *
N240 X+13 Y+0 Z-8 A+7.749 C+118.168 *
N250 X+14 Y+0 Z-8 A+7.141 C+117.071 *
N260 X+15 Y+0 Z-8 A+6.526 C+116.102 *
N270 X+16 Y+0 Z-8 A+5.907 C+115.303 *
N280 X+17 Y+0 Z-8 A+5.285 C+114.734 *
N290 X+18 Y+0 Z-8 A+4.66 C+114.488 *
N300 X+19 Y+0 Z-8 A+4.035 C+114.715 *
N310 X+20 Y+0 Z-8 A+3.413 C+115.674 *
N320 X+21 Y+0 Z-8 A+2.799 C+117.84 *
N330 X+22 Y+0 Z-8 A+2.203 C+122.176 *
N340 X+23 Y+0 Z-8 A+1.648 C+130.816 *
N350 X+24 Y+0 Z-8 A+1.196 C+148.494 *
N360 X+25 Y+0 Z-8 A+1 C+180 *
N370 X+26 Y+0 Z-8 A+1.196 C+211.506 *
N380 X+27 Y+0 Z-8 A+1.648 C+229.184 *
N390 X+28 Y+0 Z-8 A+2.203 C+237.824 *
N400 X+29 Y+0 Z-8 A+2.799 C+242.16 *
N410 X+30 Y+0 Z-8 A+3.413 C+244.326 *
N420 X+31 Y+0 Z-8 A+4.035 C+245.285 *
N430 X+32 Y+0 Z-8 A+4.66 C+245.512 *
N440 X+33 Y+0 Z-8 A+5.285 C+245.266 *
N450 X+34 Y+0 Z-8 A+5.907 C+244.697 *
N460 X+35 Y+0 Z-8 A+6.526 C+243.898 *
N470 X+36 Y+0 Z-8 A+7.141 C+242.929 *
N480 X+37 Y+0 Z-8 A+7.749 C+241.832 *
N490 X+38 Y+0 Z-8 A+8.352 C+240.635 *
N500 X+39 Y+0 Z-8 A+8.946 C+239.359 *
N510 X+40 Y+0 Z-8 A+9.533 C+238.02 *
N520 X+41 Y+0 Z-8 A+10.112 C+236.628 *
N530 X+42 Y+0 Z-8 A+10.68 C+235.192 *
N540 X+43 Y+0 Z-8 A+11.239 C+233.72 *
N550 X+44 Y+0 Z-8 A+11.788 C+232.217 *
N560 X+45 Y+0 Z-8 A+12.325 C+230.687 *
N570 X+46 Y+0 Z-8 A+12.85 C+229.134 *
N580 X+47 Y+0 Z-8 A+13.364 C+227.561 *
N590 X+48 Y+0 Z-8 A+13.864 C+225.969 *
N600 X+49 Y+0 Z-8 A+14.351 C+224.362 *
N610 X+50 Y+0 Z-8 A+14.825 C+222.741 *
N620 X+50 Y-20 Z-8 A+14.825 C+222.741 *
N630 M00 *
N640 M129 *
N650 G01 Z+150 *
N660 A+0 C+0 *
N670 X+0 Y+0 *
N680 M05 M09*
N690 G54 X+0 Y+0 Z+0 *
N700 G01 X+0 Y+0 Z+150 *
N710 M30 *
N999999 %SING G71 *
```